

## Construction of recirculating flow tank with water pumps: insight into experimental palaeontology

Takafumi TSUCHIDA\* and Yuta SHIINO\*\*

### Abstract

A flow tank with a circulatory pump system was constructed using water pumps connected with polyvinyl chloride pipes and suction hoses. The flow tank was 180 cm in length, 20 cm in width and 20 cm in height. The flow rate in the water tank was monitored by a clamp-on flowmeter, and its relevant velocity was calculated by using simple particle-tracing velocimetry. For the visualisation of the stream, a sheet laser light and small ion-exchange particle resins were used. The present recirculating experimental system realised a steady flow condition at a velocity of 7.8 cm/s or 13.0 cm/s at 5 cm from the bottom. Using the spiriferide brachiopod *Paraspirifer bownockeri* model, the present experiments reproduced the hydrodynamic properties for generating gyrating flows as observed in previous studies and found a velocity gradient and a gyrating axis position for gyrating.

*Key words:* flume experiment, pump, experimental palaeontology, biomechanics.

### Introduction

Biomechanical approaches to fossil organisms are crucial for understanding the adaptive ability and functionality that have never been observed in extant terrestrial and marine environments (Clarkson, 1975; Rayfield, 2007; Fujiwara and Hutchinson, 2012). Supplying the fossil morphology with quantitative facts, researchers could compare the results in a comprehensive way and examine how biological phenotypes have evolved in terms of biomechanical aspects within variable, extrinsic conditions. Of these approaches, experimental methods typically require a “custom-made” system for each method, unlike

---

\* Department of Geology, Faculty of Science, Niigata University, Niigata 950-2181, Japan

\*\* Graduate School of Science and Technology, Niigata University, Niigata 950-2181, Japan  
(Manuscript received 22 February, 2016; accepted 14 March, 2016)

computational simulations. One may constitute a unique experimental system corresponding to the relevant condition such as body size, ambient scale and surrounding medium.

In contrast to terrestrial organisms in a gravitational environment, aquatic organisms are influenced by the viscous medium rather than by gravity. The difference in ambient conditions occasionally results in the evolution of a hydrodynamic shape to utilise fluids for biological performance (Shiino and Kuwazuru, 2010, 2011a; Shiino and Suzuki, 2011, 2015; Shiino et al., 2012, 2014; Shiino and Angiolini, 2014). Fossil skeletal invertebrates such as trilobites and brachiopods have also been re-examined in light of biomechanical and hydrodynamic aspects, but these examinations still do not provide enough information to discuss those evolutionary scenarios in a quantitative manner. The problem begins with the construction of a custom-ordered experimental system on a scale appropriate to the organism; in turn, difficulty arises when considering the physical and biological viewpoints.

As a preliminary step in understanding the hydrodynamic properties of fossil organisms, we constructed a simple recirculating water tank system for application to a few centimetres of fossilised skeletal organisms. Using the present system and a shell spiriferide brachiopod model, we examined the validity and repeatability compared with results from previous experiments.

## Experimental procedure

A recirculating water tank system with a sheet laser light was constructed in the present study to institute a simple particle tracing method. A steady recirculating flow was generated by magnetic pumps. Using the experimental system, we examined flow behaviours around a shell model of the spiriferide brachiopod *Paraspirifer*, the hydrodynamic property that has been well demonstrated in previous studies (Shiino et al., 2009; Shiino, 2010; Shiino and Kuwazuru, 2010, 2011b).

### 1. Construction of flow tank

The water tank was 180 cm in length, 20 cm in width, and 20 cm in depth and consisted of two water pumps, JM-25H (Koshin Ltd., Japan) and SL-75N (Elepon E.C.A.P. Corporation, Japan) (Figs. 1, 2). One of the 20 cm side walls was hollowed out by a holing saw to function as a drain outlet. The outlet was directly connected via polyvinyl chloride pipes and suction hoses to the water intake of the pumps. The water from the spouts of the pumps was supplied from suction hoses on the upstream side of the water tank. A punching plate with hundreds of 5 mm holes was implemented at the upstream side of the water tank as a strainer function. The flume experiments began after filling the tank with fresh water. The water depth was maintained at a height of 15 cm throughout the experiments. The stream velocity was controlled by the combination of two pumps. Because the JM-25H water pump

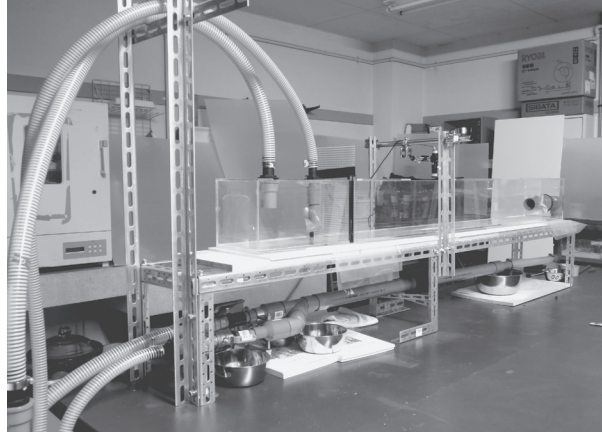


Fig. 1. Photograph of recirculating flow tank for flume experiments.

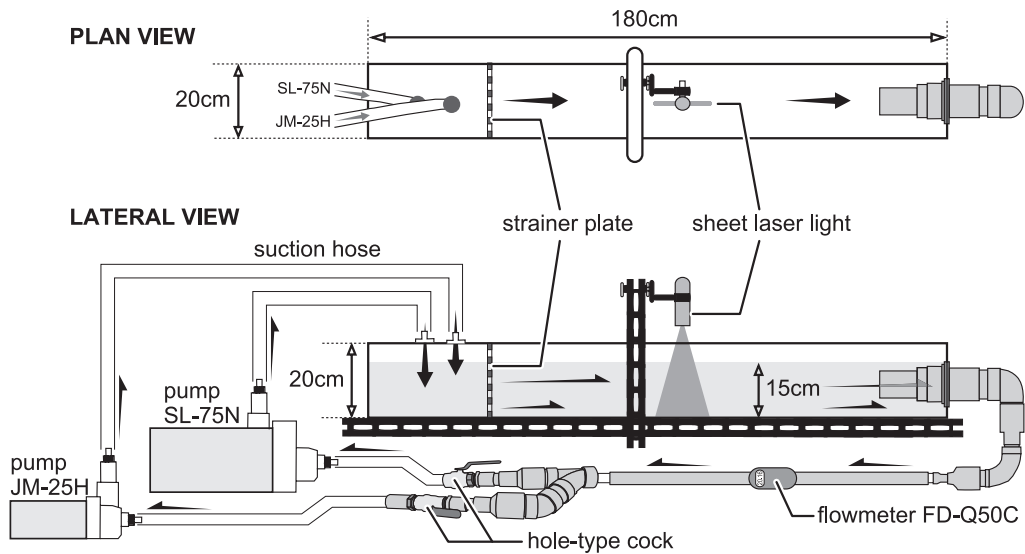


Fig. 2. Schematic illustrations of recirculating water tank with a flowmeter.

was not stable, we adopted two types of stream velocities, as follows: a slower velocity using the SL-75N and a higher velocity using both pumps. The experimental domain was set around the upstream area, 60 cm distant from the strainer plate.

A flowmeter FD-Q50C (Keyence Corporation, Japan) was clamped on the polyvinyl chloride pipe to monitor the total flow rate inside the water tank. The flowmeter analysed the average volume every 5 seconds, in litres per minute, L/min. Prior to the flume experiments using the model, the stream velocity was calculated by tracing the small particles of air bubbles.

## 2. Flow visualisations

Ion-exchange resin DIAION HP20 (Mitsubishi Chemical, Japan), which contains medium-grained particles, was used to visualise the flows inside the water tank. Each particle was  $500\ \mu\text{m}$  in average diameter, with a specific gravity of  $1.02\ \text{g}/\text{cm}^3$ . Because the ion-exchange resins were originally not water soluble, we first reduced surface groups to alcohols for dispersion into the water solution. The water solution of the ion-exchange resins was injected into the water tank using a syringe. The visualised flows were filmed by a Power Shot SX digital camera (Canon, Japan). Adjusting the settings on the digital camera, we adopted hi-vision 60 frames per second with  $1920 \times 1080$  pixels.

For the examination of the selected section within an upstream-downstream transect, we adopted a sheet laser light, which consists of a 200 mW laser light module with a wavelength of 405 nm and a cylindrical lens. The sheet laser induced fluorescence of the ion-exchange resins. The stream direction and velocity were measured by tracing the small particles of the ion-exchange resins and air bubbles moving with the fluids.

## 3. Evaluation of stream condition

For application to experimental palaeontology, an understanding of the flow conditions in the recirculating flow tank is needed. As a preliminary step, we examined stream direction and velocity within the upstream-downstream transect of median and lateral regions. To measure the stream direction and velocity, the experimental movie was translated into sequential images that filmed the luminescent particles of ion-exchange resins. The sequential images, each of which was captured every 0.05 s, were reconstructed by ImageJ image analysis software (National Institutes of Health, USA). The coordinate data from each particle was taken by a measurement function in ImageJ. Based on the coordinates of the same two particles in neighbouring images, stream direction and velocity were calculated.

Using the present experimental system, the flow patterns around the shell model of the Devonian spiriferide brachiopod *Paraspirifer bownockeri* (Stewart) were demonstrated for comparison with previous studies from our group. According to the hydrodynamic studies of spiriferides, the shell form has a role to generate spiral flows inside, enabling efficient small food particle sieving (Shiino et al., 2009; Shiino, 2010; Shiino and Kuwazuru, 2010). Identifying the function of the spiriferide shell could reveal the validity and repeatability of this experimental system. The same *Paraspirifer* model already used in Shiino et al. (2009) was attached to the bottom of the water tank with adhesive cure tape. The model was oriented with the dorsal valve facing upstream, and the flow pattern was analysed. Vector representations of the stream were drawn in Microsoft Excel (Microsoft, USA) and were composed on the first image of the sequential images.

## Results and discussion

### 1. Stream velocity

The flowmeter showed 85.5 L/min (1425 cm<sup>3</sup>/s) with the SL-75N pump in operation and 145 L/min (2417 cm<sup>3</sup>/s) with two pumps in operation (Table 1). These numerical values did not change throughout the experiments. Based on the numerical values, average flow velocities in the water tank were 4.8 cm/s and 8.1 cm/s (Table 1: Expected velocity). Using the equivalent diameter  $d_{eq}$  of the water tank, calculated as  $d_{eq} = 4dw / (2d + w)$ , where  $d$  represents the depth of water and  $w$  represents the width of the water tank, the Reynolds numbers  $Re = d_{eq}u / \nu$  (equivalent diameter  $d_{eq}$ , stream velocity  $u$  and kinematic viscosity  $\nu$ ) were approximated to be 11520 and 19440 for the velocities of 4.8 cm/s and 8.1 cm/s, respectively. For values larger than  $Re = 2000$ , it would be expected that both stream conditions were between steady and turbulent flows.

**Table 1.** Velocity conditions of the present recirculating flow tank.

Pump operation	Flow rate [L/min]	Expected velocity [cm/s]	Average velocity of stable interval [cm/s]
SL-75N	85.5	4.8	7.8
SL-75N+JM-25H	145	8.1	13.0

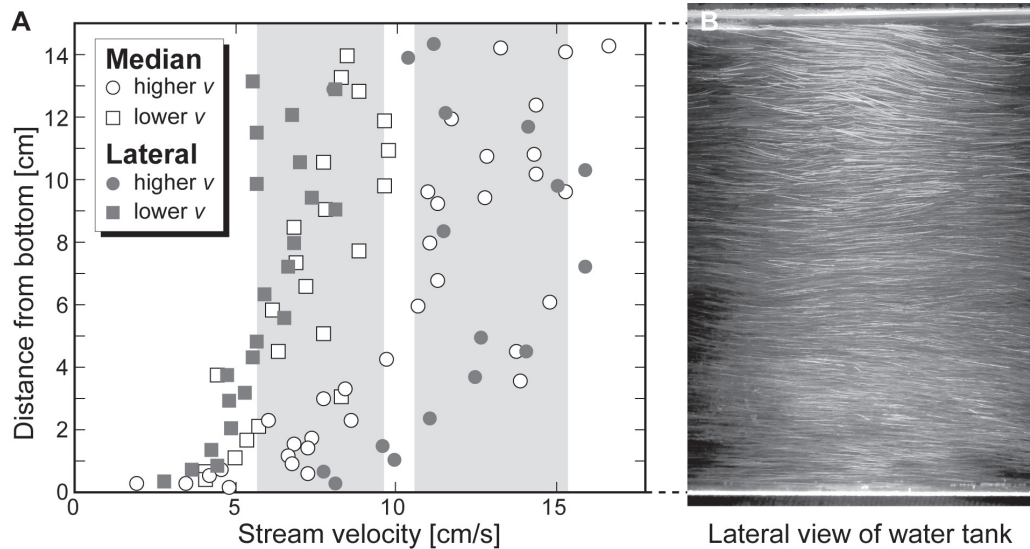


**Fig. 3.** Velocity distributions of median and lateral planes in the experimental area for two stream velocity conditions. **A.** Velocity distributions. Grey tones indicate stable intervals of velocities under the conditions of lower and higher stream velocities. **B.** Selected photograph of 0.05 s of a camera shutter opening showing the case of a median plane under the condition of a higher stream velocity. The photograph indicates that the stream was steady with no turbulent vortices.

Figure 3 shows the velocity gradient along the bottom to the top of the flow tank in median and lateral planes under the conditions of the two stream velocities. The lateral plane was set 3 cm distant from the side wall of the water tank. The local velocities of the experimental area, which were calculated by tracing the particles, differed throughout the space of the water tank (Fig. 3). Generally, the velocities were lower around the bottom level, and those of the lateral plane were also lower than the median plane (Fig. 3). Such a velocity gradient would be the result of wall friction from the water tank. In the case of the lower stream velocity, the interval between 3 to 14 cm distant from the bottom was comparatively a stable velocity condition with a maximum of velocity of 7.8 cm/s (Fig. 3; Table 1: Average velocity). In the case of the higher stream velocity, a stable interval of velocity was narrower as observed in the increase from the lower level to 5 cm above the bottom. The average velocity of this interval was 13.0 cm/s (Fig. 3; Table 1: Average velocity).

In the case of laminar flow through a pipe, it is known that the maximum velocity at the axis of pipe is twice larger than the net average velocity (Vogel, 1994). The velocity decreases close to the wall, finally reaching zero on the wall. In the present flow tank, the maximum stream velocities in all the experimental conditions were around twice the average velocities expected from the flow rate that seems to be a laminar flow. However, there is no dominant disparity of velocities between those of the median and lateral planes, suggesting the development of a turbulent boundary layer. Such an intermediate nature may be attributed to the transition conditions between the laminar and turbulent flows as estimated by the Reynolds number.

## 2. Comparison with previous studies

Figure 4 shows the vector representations of flows along the median plane view and its composite image at maximum intensity. The length of each vector indicates the velocity, and black circles are the initial luminescent points of the ion-exchange resins. The internal flows had gyrating movements with a left-to-right axis direction, as shown in our previous studies (Fig. 4; Shiino et al., 2009; Shiino, 2010; Shiino and Kuwazuru, 2010). The velocities of the gyrating flows moving downward along the inner surface of the ventral valve were considerably higher than those moving upward along the dorsal valve (Fig. 4A). The centre of the gyrating axis was a lateral gape located slightly above the bottom (Fig. 4B, C).

The difference in gyrating velocities within the shell model may be attributed to the shell function to generate passive flows. Based on previous studies from our group, the spiriferide sulcus, a major depression along the midline of the shell, functions to obtain a higher pressure around the sulcus gape (Shiino and Kuwazuru, 2010). This pressurisation results in the inflow through the sulcus gape and the outflows through the right and left lateral gapes (Shiino et al., 2009). Consequently, a flow velocity immediately after the inflow

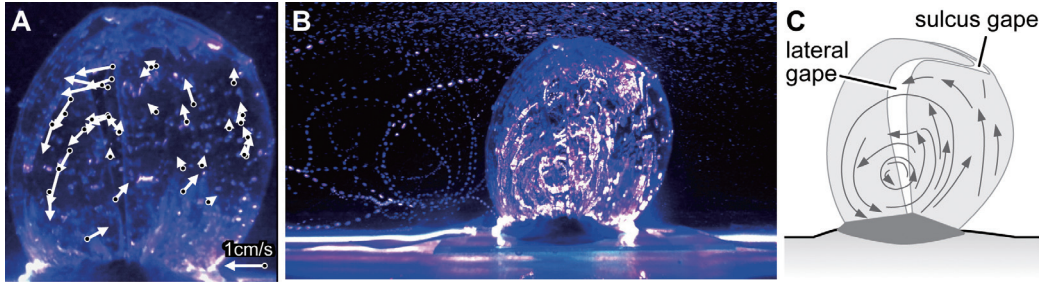


**Fig. 4.** Flow behaviours for the shell model of spiriferide brachiopod *Paraspirifer bownockeri*. **A.** Vector representations of flows inside the model. The vectors realised a vortex movement and its velocity gradient inside the model. **B.** Composite image of maximum brightness. Sequential images of 10 s were merged into one image to extract the brightest pixel. **C.** Schematic illustration of B. Drawing the luminescent particles allowed visualisation of the gyration motion of flows inside the model. The gyration axis was on the projection of the lateral gape slightly above the bottom.

through the sulcus gape was higher than any of the others. The present results indicate that our experimental system determined the velocity gradient of the gyration flows, as has been demonstrated previously by the computational fluid dynamics simulation.

### 3. Future perspectives of the present recirculating system and its application

The present study reconstructed the recirculating flow tank with mechanical water pumps. This flume experimental system could realise a steady flow condition with a stream velocity of 7.8 cm/s or 13.0 cm/s, 5 cm distant from the bottom. Although the present recirculating flow tank demonstrated only two types of stream velocities at this time, in the future, it can be improved to install additional pumps and voltage regulators. The present experimental system could be applicable for understanding the hydrodynamic properties of skeletal organisms with small to moderate sizes less than 10 cm such as brachiopods.

There still remain problems on the visualisations of flows. As is clear from the results shown in Fig. 4, the refractive index of the model inhibited the ability to obtain a clear image; the ion-exchange resin particles seem to be fogged by halation or refraction. In addition, the air-water interface of the flow tank refracted the sheet laser light, and thus, the luminescence of visualised particles was not stable. Further improvements of model construction and laser lighting conditions may provide a rigorous experimental method to find quantitative biomechanical features in fossilised aquatic organisms.

### Acknowledgements

We gratefully acknowledge Hiroshi Kurita for helpful support of experimental facilities. We thank Hayato Ueta, Atsushi Matsuoka, Toshiyuki Kurihara and Isao Niikawa for their thorough discussions. This study was financially supported in part by the Uchida Energy

Science Promotion Foundation, by the Sasakawa Scientific Research Grant from the Japan Science Society and by the JSPS KAKENHI Grant Numbers 25630047 and 26400503.

### References

- Clarkson, E. N. K., 1975, The evolution of the eye in trilobites. *Fossils and Strata*, **4**, 7–31.
- Fujiwara, S. and Hutchinson, J. R., 2012, Elbow joint adductor moment arm as an indicator of forelimb posture in extinct quadrupedal tetrapods. *P. Roy. Soc. B-Biol. Sci.*, **279**, 2561–2570.
- Rayfield, E. J., 2007, Finite element analysis and understanding the biomechanics and evolution of living and fossil organisms. *Annu. Rev. Earth. Pl. Sci.*, **35**, 541–576.
- Shiino, Y., 2010, Passive feeding in spiriferide brachiopods: an experimental approach using models of Devonian *Paraspirifer* and *Cyrtospirifer*. *Lethaia*, **43**, 223–231.
- Shiino, Y. and Angiolini, L., 2014, Hydrodynamic advantages in the free-living spiriferinide brachiopod *Pachycyrtella omanensis*: functional insight into adaptation to high energy flow environment. *Lethaia*, **47**, 216–228.
- Shiino, Y. and Kuwazuru, O., 2010, Functional adaptation of spiriferide brachiopod morphology. *J. Evolution. Biol.*, **23**, 1547–1557.
- Shiino, Y. and Kuwazuru, O., 2011a, Comparative experimental and simulation study on passive feeding flow generation in *Cyrtospirifer*. *Mem. Assoc. Australas. Palaeontologists*, **41**, 1–8.
- Shiino, Y. and Kuwazuru, O., 2011b, Theoretical approach to the functional optimisation of spiriferide brachiopod shell: Optimum morphology of sulcus. *J. Theor. Biol.*, **276**, 192–198.
- Shiino, Y., Kuwazuru, O., Suzuki, Y. and Ono, S., 2012, Swimming capability of the remopleurid trilobite *Hypodicranotus striatus*: Hydrodynamic functions of the exoskeleton and the long, forked hypostome. *J. Theor. Biol.*, **300**, 29–38.
- Shiino, Y., Kuwazuru, O., Suzuki, Y., Ono, S. and Masuda, C., 2014, Pelagic or benthic? Mode of life of the remopleurid trilobite *Hypodicranotus striatulus*. *B. Geosci.*, **89**, 207–218.
- Shiino, Y., Kuwazuru, O. and Yoshikawa, N., 2009, Computational fluid dynamics simulations on a Devonian spiriferid *Paraspirifer bownockeri* (Brachiopoda): Generating mechanism of passive feeding flows. *J. Theor. Biol.*, **259**, 132–141.
- Shiino, Y. and Suzuki, Y., 2011, The ideal hydrodynamic form of the concavo-convex productide brachiopod shell. *Lethaia*, **44**, 329–343.
- Shiino, Y. and Suzuki, Y., 2015, A rectifying effect by internal structures for passive feeding flows in a concavo-convex productide brachiopod. *Paleontol. Res.*, **19**, 283–287.
- Vogel, S., 1994, *Life in Moving fluids*. Princeton University Press, Princeton, 467p.